Pamphlet 3

ABSORBED FRACTIONS FOR PHOTON DOSIMETRY

G. L. Brownell, W. H. Ellett and A. R. Reddy*

1. INTRODUCTION

Traditionally the calculation of photon exposure has been performed by the integration of a point-source kernel consisting of simple inverse-square and exponential attenuation factors and the results expressed in roentgen. The accuracy of this type of approximation is limited because such simple kernels cannot adequately consider the dose from scattered radiation or the effects of boundaries. For internal emitters, the calculation of absorbed dose in rads is preferred to a dose calculation expressed as a roentgen exposure in air. Recent calculations of buildup factors and new techniques for treating boundary problems by means of Monte Carlo sampling have improved the methods of calculating the photon dose directly in rads. These methods rigorously consider the contribution to the absorbed dose from both direct and scattered radiation and give results in a form directly applicable to absorbed-dose calculation.

While the results obtained with these newer methods do not differ greatly from those obtained with simple exponential kernels for initial photon energies greater than a few tenths of an MeV, estimates of the absorbed dose are significantly different for photons of lower energy. It is perhaps the increased use of low-energy photon emitters in clinical practice that has provided the chief impetus for the development of exact photon-scattering calculations for dosimetry problems.

Monte Carlo calculation of photon diffusion provides a direct and accurate means of calculating absorbed dose from internal photon emitters in situations where the source and absorber geometries are defined. Calculations have been carried out for point and uniform-source distributions within bounded, tissue-equivalent material. The photon *absorbed fraction* ϕ is simply the fraction of the emitted photon energy that is absorbed in the region of interest (*1–3*). It is clear that the absorbed fraction can be determined only after specifying the source and absorber geometry, the photon energy and the intervening material. Results of such calculations are presented in this pamphlet for a sufficient number of geometries and energies to permit accurate interpolation. More recently the term *specific absorbed fraction* Φ has been proposed to represent the absorbed fraction per gram of absorbing medium (*4*).

2. CALCULATION OF ABSORBED DOSE

As stated above, the photon absorbed fraction can be expressed as

$$\phi = \frac{\text{photon energy absorbed by target}}{\text{photon energy emitted by source}}, \qquad (1)$$

The source may be a point, line, surface or volume. The target volume may or may not enclose the source, and the target volume may, under certain conditions of common clinical interest, be the same as the source volume.

The quantity of photon energy emitted by a source depends on the source activity and the energy of the emitted photons. In general, a radionuclide will have more than one photon energy component in its decay scheme. Since the scattering and absorption of photons is energy dependent, each energy component must be considered separately. It is convenient in absorbed-dose calculations to use for each photon component (as well as for particulate radiations, ref. 4) an equilibrium absorbed-dose constant Δ_i which gives the total energy in g-rad/μCi-h emitted by that component. The equilibrium absorbed-dose constant for a photon of fractional abundance n_i in photons emitted (corrected

* Special consultant to MIRD.

TABLE 1. EQUILIBRIUM ABSORBED DOSE CONSTANT FOR AN INFINITE TISSUE-LIKE MEDIUM*

Radionuclide	Half-Life	Principal energy components (MeV)	n_i fractional abundance of photon (No./dis.)	Δ_i (g-rad/μCi-h)
^{22}Na†	2.58 y	0.511	1.80	1.959
		1.277	0.99	2.693
^{24}Na	15 h	1.37	1.00	2.918
		2.753	1.00	5.864
^{47}Ca	4.7 d	0.48	0.06	0.061
		0.83	0.06	0.106
		1.31	0.77	2.149
^{47}Sc	3.4 d	0.161	0.60	0.206
^{51}Cr	27.8 d	0.006 (x-ray)	0.91	0.0116
		0.324	0.09	0.062
^{59}Fe	45 d	0.145	0.008	0.002
		0.191	0.025	0.010
		0.337	0.003	0.002
		1.102	0.56	1.314
		1.290	0.44	1.209
^{60}Co	5.27 y	1.172	0.99	2.472
		1.332	0.99	2.809
^{99m}Tc	6.0 hr	0.002	0.986	0.0042
		0.0183 (x-ray)	0.046	0.00177
		0.0206 (x-ray)	0.010	0.00045
		0.140	0.90	0.268
		0.142	0.004	0.00122
^{123}I	13 hr	0.027 (x-ray)	1.04	0.0596
		0.1595	1.00	0.340
		0.53	0.02	0.028
^{125}I	60.0 d	0.027 (x-ray)	1.126	0.0657
		0.031 (x-ray)	0.242	0.0160
		0.035	0.07	0.00522
^{131}I	8.05 d	0.080	0.022	0.004
		0.284	0.053	0.032
		0.364	0.82	0.637
		0.638	0.09	0.122
		0.724	0.03	0.046
^{133}Xe	5.27 d	0.029 (x-ray)	0.60	0.0371
		0.081	0.40	0.069
		0/160	0.001	0.003
^{137}Cs	30 y	0.032 (x-ray)	0.07	0.0048
		0.6616	0.85	1.199
^{197}Hg	65 hr	0.068 (x-ray)	0.57	0.0828
		0.077	0.20	0.0329
		0.079 (x-ray)	0.18	0.0302
		0.191	0.01	0.0041
^{198}Au	64.8 hr	0.069 (x-ray)	0.027	0.004
		0.41177	0.95	0.834
		0.6758	0.01	0.014
		1.086	0.002	0.005
^{203}Hg	47 d	0.073 (x-ray)	0.15	0.0233
		0.279	0.81	0.481
Radium‡				3.31

* Decay schemes used in these calculations are taken from Handbook of Physics and Chemistry (1966-1967), Radiological Handbook (1960) and Nuclear Data Sheets. Characteristic x-radiation of the daughter nuclide that accompanies the orbital electron capture and the internal conversion process is entered under the respective parent nuclide wherever significant.

† Includes annihilation radiation.

‡ ^{226}Ra and decay products with 0.5 mm platinum filter; H. E. Johns 1953.

for internal conversion) per disintegration, and energy $\bar{E}_i$ in MeV, will be

$$\Delta_i = 1.602 \times 10^{-6}\left(\frac{\text{erg}}{\text{MeV}}\right) \times 10^{-2}\left(\frac{\text{rad}}{\text{erg-g}}\right) \times 3.70 \times 10^{4}\left(\frac{\text{dis/sec}}{\mu\text{Ci}}\right) \times 3.60 \times 10^{3}\left(\frac{\text{sec}}{\text{h}}\right) \times n_i\bar{E}_i\left(\frac{\text{MeV}}{\text{dis}}\right),$$

$$\Delta_i = 2.13\ n_i\bar{E}_i \quad \text{g-rad}/\mu\text{Ci-h}. \tag{2}$$

Table 1 lists values of Δ_i for the photons of several commonly used radionuclides.

The photon energy absorbed per μCi-h by the target is the product of the photon absorbed fraction and the equilibrium absorbed-dose constant. For a source emitting photons of different energies, the average absorbed dose $\bar{D}$ from penetrating photon radiations delivered to a target of mass m in g is

$$\bar{D} = \frac{\tilde{A}}{m}\sum_i \phi_i \Delta_i \quad \text{rad}, \tag{3}$$

where $\tilde{A}$ is the cumulated activity in μCi-h and ϕ_i is the absorbed fraction for the particular target volume, source location and photon energy. It is often desired to calculate the average absorbed dose rate, $\bar{R}$:

$$\bar{R} = \frac{A}{m}\sum_i \phi_i \Delta_i \quad \text{rad/h} \tag{4}$$

where A is the activity in μCi.

Equation 4 is equally valid for point, line, surface or volume distributions of activity providing A is the total activity in the source region. A commonly encountered situation occurs when the source volume is the same as the target volume, as in the case of the self dose from an internal distribution of radioactivity. In this case Equation 4 can be re-written as

$$\bar{R} = C\sum_i \phi_i \Delta_i \quad \text{rad/h}, \tag{5}$$

where C is the concentration of activity in μCi/g.

3. GENERATION OF ABSORBED FRACTION DATA

In general, absorbed fractions for finite media must be calculated by means of Monte Carlo techniques. This is performed by expressing the equations for photon scattering and absorption as probability distributions, normalizing these probability distributions so that they can be sampled efficiently using a series of random numbers having a uniform distribution, and then sampling the probability distributions an appropriate number of times to determine the average energy lost in successive interactions by source photons. Since photon diffusion is treated stepwise in these calculations, it is possible to include the effects of

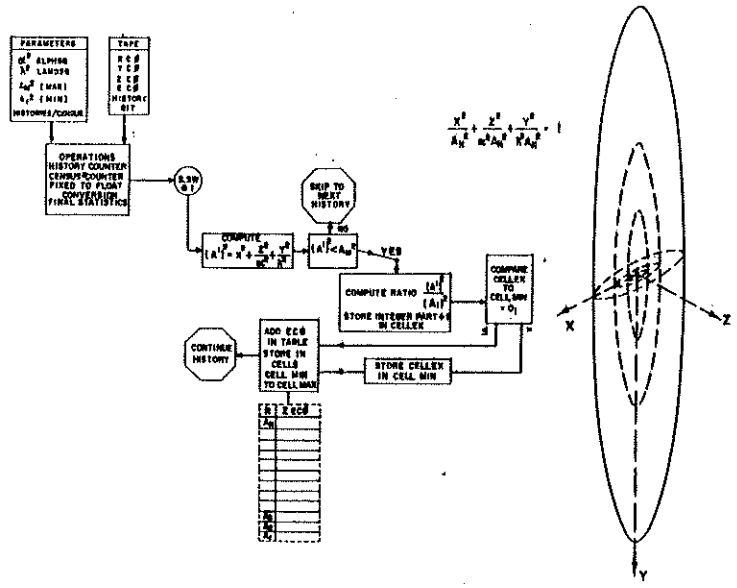

FIG. 1. Simplified flow diagram of a Sort program for target volumes of ellipsoidal shape of semi-major axes $a_1, \ldots a_n$ shown at right. (Courtesy of *Brit. J. Radiol.*)

boundaries. The number of photon histories required to give meaningful results depends on both the energy of the photon and on the target geometry.

As a practical matter, to reduce computer costs, almost all of our machine computations of absorbed fractions have been performed in two parts, a Monte Carlo and a separate Sort program. The Monte Carlo program is used to simulate photon diffusion. The Sort program is to calculate absorbed fractions from the Monte Carlo results.

In the Monte Carlo program the initial direction of a source photon is selected by means of internally generated random numbers to simulate an isotropic source. The distance the photon travels before its first interaction is found by sampling the exponential probability distribution appropriate to the energy of the photon, and the new position coordinates are calculated. Next, the type of interaction is selected randomly with probabilities proportional to the ratios of the photoelectric and Compton cross sections to the total scattering cross section. If a photoelectric event is indicated, the photon history is terminated and the position coordinates and energy transfer are recorded. If a Compton interaction is indicated, the Klein Nishina scattering distribution is sampled using a method originated by H. Kahn (5) to determine the energy transfer and scattering angle. The energy lost to the Compton electron and the position coordinates of the interaction are recorded, and the history continued with a randomly chosen azimuthal scattering angle. Histories are continued until a photoelectric event takes place, or the energy of the scattered quanta is less than 10 keV.

The basic Monte Carlo data of position coordinates and energy transfer are stored on magnetic tapes, each tape containing 40,000 to 125,000 independent photon histories. These tapes are used as input data for a family of Sort programs which determine absorbed fractions by simply adding the energy losses in various target volumes (*1*). A typical Sort program is illustrated by the flow diagram shown in Fig. 1, where a point source in the center of a concentric array of ellipsoidal targets is indicated.

As illustrated in Fig. 1, a set of position coordinates is used to determine the largest ellipsoid within which a given interaction has occurred. The energy loss associated with this interaction is added to all ellipsoids containing the interaction if certain criteria are met. The logic of the program is such that the energy transfer from photons coming from outside the boundary of an ellipsoid is excluded from the tabulation of energy transfer to that ellipsoid. In this way contributions from backscattered photons are not included in the calculation of absorbed fraction.

Monte Carlo calculations of the energy absorbed by each target volume are subject to statistical fluctuations. The amount of this variation is determined by dividing the total sample of 40,000 to 125,000 histories into censii containing several thousand histories and calculating the absorbed fraction for each census. The standard deviation of the mean absorbed fraction for each target volume is calculated internally by the Sort program. As would be expected, the statistical variation is dependent on the target volume, being larger for the smaller phantoms which contain fewer interactions. Typically, the standard deviation of the mean for the smallest target of a given set is from 1 to 2%. For the larger targets, 0.1–0.2% is typical.

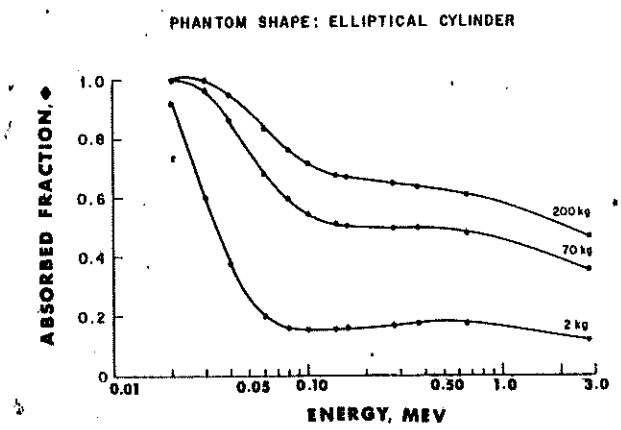

FIG. 2. Variation of absorbed fraction with energy and mass for elliptical cylinders, central point source.

The absolute error of the absorbed fractions is larger than that due to the sampling variation since the absorption coefficients on which the calculations are based have an uncertainty of at least 2% (*6,7*).

The logic of the Monte Carlo program assumes that scattered photons of less than 10 keV are absorbed by the photoelectric effect at the point of their last Compton interaction. Recent Monte Carlo studies of the spectral distribution of scattered photons have shown that the use of this 10 keV cutoff has no effect on the calculated values of absorbed fraction (*8*). Recent studies indicate that the effects of coherent scatter on absorbed fraction are small (*8*), and it is neglected in our calculations. Pair production is also not considered in our calculations because its cross section in low atomic number materials at the maximum energy (2.75 MeV) for which absorbed fractions are reported here is so small that the error introduced by neglecting pair production is less than 1%.

Sort programs are used to calculate the absorbed fraction in simplified unit-density target geometries that approximate anatomical shapes. The models that have been studied include ellipsoids, elliptical cylinders, right circular cylinders and spheres.

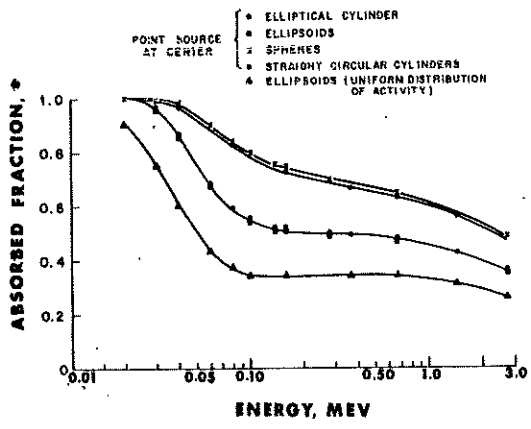

FIG. 3. Variation of absorbed fraction with energy and target geometry, 70 kg target mass.

4. VARIATION OF ABSORBED FRACTION BETWEEN TARGETS OF DIFFERENT MASS AND IDENTICAL SHAPE

The variation of absorbed fraction with initial photon energy for central point sources in elliptical cylinders is shown in Fig. 2. It is seen that for small values of mass, the absolute value of the absorbed fraction is not very sensitive to variations in initial photon energy between 0.1 MeV and 1 MeV. This is because the increased transmission of high-energy photons is largely compensated by the increased energy transfer from first-collision Compton events. In larger target volumes, direct transmission of primary photons is less, and the absorbed fraction is more energy dependent. For all target sizes, the absorbed fraction approaches unity at low energies since the photoelectric process dominates energy transfer in this region. The exact relationship between target mass and absorbed fraction depends on the target shape. However, results similar to those given in Fig. 2 are observed with all target geometries. Although the conclusions here refer specifically to point sources at the center of target volumes, similar behavior is observed for a uniform distribution of activity or for point sources at other locations.

5. VARIATION OF ABSORBED FRACTION BETWEEN TARGETS OF DIFFERENT SHAPE AND IDENTICAL MASS

The variation of absorbed fraction with initial photon energy for different target geometries having a 70-kg mass is shown in Fig. 3. The relative dimensions for the different target geometries used for these curves are the same as those used in Tables 4–6 and 9.

The ellipsoids and the elliptical cylinders for which the absorbed fractions are shown in this figure have the same maximum cross section dimensions. The ellipsoidal target is, however, 50% higher. Notwithstanding this difference in height, the absorbed fractions for central point sources in ellipsoids and elliptical cylinders are almost identical. Note, however, that for uniform distribution of activity the absorbed fractions for ellipsoids are significantly less than those for elliptical cylinders.

Therefore, for centrally located sources in the trunk of the body, the use of an elliptical cylinder as a model for total-body absorbed-dose calculation is justifiable regardless of the patient's height. In the case of uniformly distributed activity in the body, an ellipsoidal model is a better approximation for calculation of total-body absorbed-dose since the human figure tapers toward the head and feet.

Spherical target volumes have a larger average radius than elongated targets of equal mass. The

absorbed fraction for spherical targets is therefore larger than for elongated targets for both point source and uniform distribution of activity.

6. ABSORBED FRACTIONS FOR FINITE SPHERICAL TARGETS IN AN INFINITE MEDIUM

It is sometimes of interest to determine the absorbed fraction from point sources for finite target volumes located in a larger volume of scattering material. The absorbed fraction in this case must include the back-scattered radiation from the surrounding medium. Figure 4 shows the results of such calculations. These curves give the radius of a sphere surrounding a point source required to absorb 50% and 90% of the emitted photon energy. Figure 5 shows the absorbed fractions for spheres of various radii in an infinite medium as a function of energy. The data shown in Figs. 4 and 5 can be used to obtain curves of energy absorption as a function of distance for point sources of various radionuclides in infinite tissue media. The same data can also be used to calculate specific absorbed fractions Φ at various distances from a point source. However, it is more accurate to use Monte Carlo histories to calculate the intensity of the radiation at the point of interest and then obtain specific absorbed fraction from calculated energy fluence (*8*).

7. ABSORBED FRACTION: COMPARISON OF MONTE CARLO AND MOMENTS METHOD RESULTS

Since most of our calculations have been for finite targets, the results shown in Figs. 4 and 5 for an unbounded medium are the only Monte Carlo results we have obtained that are suitable for comparison with M. Berger's moments-method results, presented in MIRD Pamphlet No. 2 (*9*). Berger's results are for water while ours are for a tissue composition having slightly different absorption and scattering cross sections. These effects can be reduced by expressing both sets of results in terms of mean free paths, the reciprocal of the total attenuation coefficients used in the respective calculations. The Monte Carlo data shown in Table 2 has been interpolated from curves such as shown in Figs. 4 and 5 to present results for the photon energies studied by Berger. The last digit shown in our results is not very significant because of graphical interpolation. However, it is seen that the two methods give comparable results.

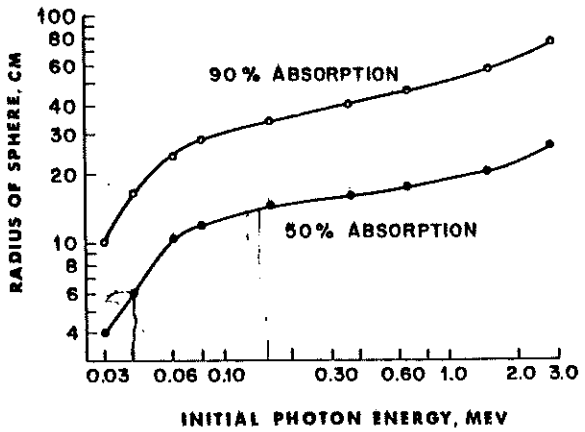

FIG. 4. Radius of sphere needed to absorb 50% and 90% of the emitted photon energy from a central point source in an infinite tissue medium.

The Monte Carlo Code used for calculating the absorbed fractions presented in this pamphlet have been compared to the absorbed fractions as determined by a Code devised by Snyder and Ford (*10*). The result of this comparison for the limited cases studied was quite good (*11*).

8. DOSE RECIPROCITY THEOREM

The absorbed dose delivered at the center of a target containing a uniform distribution of activity is greater than the average absorbed dose received by the target. Application of the dose reciprocity theorem allows specific absorbed fractions at the center of a uniform distribution of activity to be calculated by dividing the appropriate central point source absorbed fraction

TABLE 2. COMPARISON OF MONTE CARLO (MGH) AND MOMENTS METHOD (NBS) RESULTS*

	mfp for 50% absorption		mfp for 90% absorption	
E(MeV)	MGH	NBS / MGH	MGH	NBS / MGH
2.0	1.15	1.01	3.32	1.01
1.0	1.36	0.99	3.74	1.00
0.5	1.58	1.01	4.16	1.01
0.1	2.15	1.01	5.02	1.00
0.08	2.16	0.98	5.04	0.97
0.06	1.98	0.96	4.64	0.98
0.04	1.52	0.96	3.84	0.98
0.03	1.19	0.96	3.30	0.97

* Radius in mean free paths required to absorb 50% and 90% of energy emitted by a point source in an infinite medium.

TABLE 3. TISSUE COMPOSITION USED IN ABSORBED-FRACTION CALCULATIONS

Element	% mass
Oxygen	71.39
Carbon	14.89
Hydrogen	10.00
Nitrogen	3.47
Chlorine	0.10
Sodium	0.15

TABLE 4. ABSORBED FRACTIONS FOR CENTRAL POINT SOURCES IN ELLIPTICAL CYLINDERS OR ELLIPSOIDS*

	φ													
Mass (kg)	0.020 MeV	0.030 MeV	0.040 MeV	0.060 MeV	0.080 MeV	0.100 MeV	0.140 MeV	0.160 MeV	0.279 MeV	0.364 MeV	0.662 MeV	1.460 MeV	2.750 MeV	Radium†
2	0.924	0.605	0.367	0.203	0.166	0.159	0.160	0.161	0.171	0.176	0.176	0.157	0.125	0.163
4	0.956	0.697	0.453	0.263	0.212	0.202	0.200	0.201	0.214	0.218	0.216	0.193	0.154	0.201
6	0.971	0.749	0.509	0.305	0.247	0.233	0.229	0.230	0.242	0.245	0.243	0.217	0.174	0.227
8	0.980	0.785	0.551	0.340	0.276	0.258	0.252	0.253	0.265	0.267	0.263	0.236	0.190	0.247
10	0.985	0.811	0.585	0.368	0.301	0.280	0.272	0.272	0.283	0.285	0.281	0.252	0.204	0.263
20	0.995	0.881	0.689	0.468	0.388	0.358	0.342	0.340	0.348	0.348	0.340	0.306	0.251	0.320
30	0.998	0.914	0.749	0.534	0.447	0.413	0.391	0.387	0.391	0.389	0.379	0.341	0.282	0.357
40	0.998	0.934	0.788	0.581	0.491	0.456	0.429	0.423	0.424	0.421	0.409	0.368	0.306	0.385
50	0.999	0.946	0.817	0.619	0.527	0.491	0.460	0.453	0.450	0.447	0.433	0.390	0.325	0.408
60	0.999	0.956	0.838	0.649	0.557	0.520	0.487	0.478	0.473	0.469	0.453	0.409	0.342	0.427
70	0.999	0.963	0.855	0.674	0.583	0.545	0.511	0.500	0.493	0.488	0.471	0.425	0.356	0.444
80	0.999	0.968	0.869	0.696	0.606	0.567	0.532	0.520	0.511	0.505	0.486	0.439	0.369	0.458
90	0.999	0.972	0.881	0.715	0.626	0.587	0.551	0.538	0.527	0.520	0.500	0.452	0.380	0.471
100	0.999	0.976	0.890	0.731	0.643	0.604	0.568	0.554	0.542	0.534	0.513	0.463	0.391	0.483
120	0.999	0.981	0.906	0.759	0.674	0.634	0.597	0.583	0.567	0.558	0.535	0.483	0.409	0.505
140	0.999	0.985	0.918	0.782	0.700	0.660	0.622	0.607	0.589	0.579	0.555	0.501	0.425	0.523
160	0.999	0.987	0.928	0.801	0.722	0.681	0.644	0.629	0.609	0.598	0.572	0.516	0.439	0.539
180	0.999	0.989	0.936	0.818	0.740	0.700	0.662	0.648	0.627	0.615	0.587	0.530	0.452	0.554
200	0.999	0.990	0.944	0.833	0.756	0.717	0.678	0.665	0.643	0.630	0.601	0.542	0.463	0.568

* The principal axes of the elliptical cylinders and the ellipsoids are in the ratios of 1/1.8/6.19 and 1/1.8/9.27, respectively.
† Weighted value for ^{226}Ra decay product spectrum given by H. E. Johns, 1953.

TABLE 5. ABSORBED FRACTIONS FOR CENTRAL POINT SOURCES IN SPHERES

	φ									
Mass (kg)	0.020 MeV	0.030 MeV	0.040 MeV	0.060 MeV	0.100 MeV	0.140 MeV	0.160 MeV	0.279 MeV	0.662 MeV	2.750 MeV
2	0.989	0.794	0.537	0.322	0.243	0.233	0.234	0.241	0.235	0.168
4	0.996	0.878	0.658	0.421	0.317	0.301	0.297	0.302	0.293	0.209
6	0.999	0.916	0.727	0.488	0.370	0.348	0.342	0.344	0.330	0.238
8	0.999	0.938	0.772	0.540	0.413	0.386	0.379	0.377	0.359	0.259
10	0.999	0.952	0.806	0.581	0.448	0.418	0.409	0.405	0.382	0.277
20	0.999	0.982	0.894	0.709	0.569	0.529	0.517	0.500	0.461	0.339
30	0.999	0.991	0.932	0.780	0.644	0.600	0.587	0.562	0.514	0.380
40	0.999	0.995	0.954	0.826	0.698	0.652	0.639	0.608	0.554	0.411
50	0.999	0.996	0.966	0.859	0.738	0.692	0.679	0.644	0.586	0.436
60	0.999	0.997	0.974	0.882	0.770	0.725	0.712	0.675	0.613	0.457
70	0.999	0.998	0.980	0.900	0.796	0.752	0.739	0.700	0.637	0.476
80	0.999	0.998	0.983	0.915	0.818	0.775	0.762	0.722	0.657	0.492
90	0.999	0.999	0.986	0.926	0.836	0.794	0.781	0.741	0.675	0.507
100	0.999	0.999	0.988	0.935	0.851	0.811	0.799	0.758	0.691	0.520
120	0.999	0.999	0.991	0.948	0.876	0.839	0.827	0.786	0.719	0.544
140	0.999	0.999	0.993	0.958	0.895	0.860	0.849	0.809	0.742	0.564
160	0.999	0.999	0.995	0.965	0.910	0.878	0.867	0.829	0.761	0.582
180	0.999	0.999	0.996	0.971	0.923	0.892	0.882	0.845	0.778	0.598
200	0.999	0.999	0.998	0.976	0.933	0.904	0.894	0.858	0.792	0.612

by the target mass. The dose reciprocity theorem states that the absorbed dose delivered to a point from a uniform-volume distribution of activity is equal to the average absorbed dose delivered to that volume by the same amount of activity concentrated at that point (*4,12,13*). Using exact scattering calculations at 0.040 and 0.662 MeV, Ellett, Callahan and Brownell (*2*) have shown that the reciprocity theorem holds for the case of a 2.2-kg centrally located region within a 70-kg target. It is expected that for most regions of activity within the trunk use of the dose reciprocity theorem will give acceptable results. The dose reciprocity theorem extends the usefulness of the point-source absorbed-fraction data. For example, the absorbed

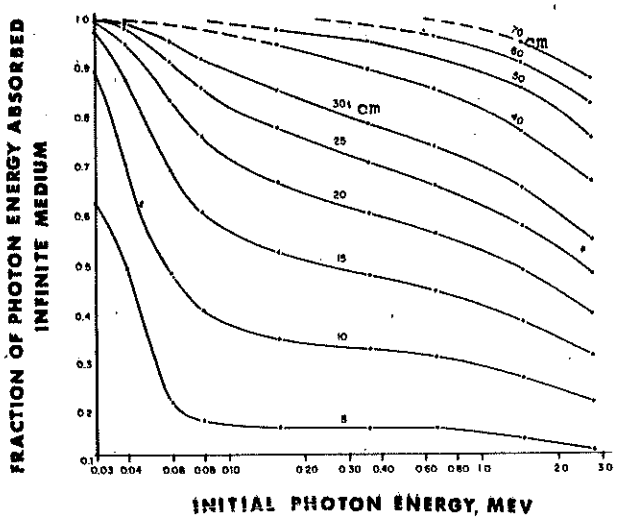

FIG. 5. Fraction of photon energy from point sources absorbed in spheres of different radii in an infinite tissue medium.

fractions obtained for various source positions along the central axis of an elliptical cylinder can be used to determine the absorbed dose at points along the central axis (e.g., gonadal dose) from a uniform distribution of activity in the target.

9. SCALING OF THE ABSORBED FRACTION FOR DIFFERENT MASS DENSITIES AND ELECTRON DENSITIES

All of the calculations of absorbed fraction presented here (except for Table 7) refer to a unit-density tissue composition as shown in Table 3. The electron density of the mixture is 3.308×10^{23} electrons/g. Our studies indicate that 0.25% by weight of sodium chloride has little effect on the value of the absorbed fraction below 40 keV, i.e., less than 1%. For initial energies greater than 40 keV, trace constituents having an atomic number of less than 18 have a negligible effect on the absorbed fraction. It should be noted that at some energies the results given in Tables 4–9 differ slightly from those we have previously published (*1,2*) for a tissue having an electron density of 3.41×10^{23} electrons/g.

The density of the tissue-equivalent material used in all calculations is unity. For material of identical atomic composition but density other than unity, the values of absorbed fraction presented in Tables 4–10

TABLE 6. ABSORBED FRACTIONS FOR CENTRAL POINT SOURCES IN RIGHT CIRCULAR CYLINDERS*

Mass (kg)	ϕ 0.040 MeV	0.080 MeV	0.160 MeV	0.364 MeV	0.662 MeV	1.460 MeV
2	0.528	0.258	0.224	0.240	0.229	0.200
4	0.645	0.336	0.290	0.295	0.288	0.253
6	0.712	0.391	0.335	0.333	0.326	0.286
8	0.757	0.435	0.370	0.363	0.354	0.311
10	0.789	0.471	0.399	0.387	0.376	0.332
20	0.878	0.593	0.501	0.472	0.453	0.401
30	0.917	0.668	0.568	0.528	0.504	0.446
40	0.940	0.721	0.618	0.571	0.543	0.480
50	0.954	0.761	0.658	0.605	0.575	0.509
60	0.964	0.792	0.691	0.633	0.602	0.533
70	0.971	0.818	0.719	0.658	0.625	0.553
80	0.977	0.838	0.743	0.679	0.646	0.572
90	0.981	0.856	0.763	0.698	0.664	0.588
100	0.984	0.871	0.781	0.714	0.680	0.603
120	0.989	0.894	0.811	0.742	0.708	0.629
140	0.992	0.911	0.834	0.765	0.730	0.651
160	0.994	0.924	0.852	0.784	0.749	0.669
180	0.994	0.933	0.866	0.800	0.765	0.685
200	0.994	0.939	0.877	0.813	0.777	0.698

* The principal axes of the right circular cylinders are in the ratio of 1/1/0.75.

TABLE 7. ABSORBED FRACTIONS FOR CENTRAL POINT SOURCES IN RIGHT CIRCULAR CYLINDERS*

Height (cm)	Radius (cm) 3	5	10
		0.040 MeV	
5	0.219	0.299	0.379
10	0.266	0.403	0.582
15	0.279	0.442	0.682
20	0.283	0.458	0.731
		0.080 MeV	
5	0.092	0.128	0.174
10	0.113	0.179	0.292
15	0.119	0.200	0.365
20	0.122	0.210	0.409
		0.160 MeV	
5	0.095	0.128	0.168
10	0.115	0.170	0.261
15	0.122	0.189	0.318
20	0.129	0.198	0.353
		0.364 MeV	
5	0.103	0.137	0.183
10	0.124	0.180	0.268
15	0.131	0.199	0.318
20	0.134	0.208	0.348
		0.662 MeV	
5	0.104	0.140	0.185
10	0.124	0.181	0.265
15	0.131	0.199	0.311
20	0.134	0.208	0.339
		1.460 MeV	
5	0.093	0.124	0.165
10	0.111	0.160	0.234
15	0.117	0.175	0.273
20	0.120	0.184	0.298

* These data were obtained for Dr. G. K. Bahr of Cincinnati General Hospital and are presented here through his courtesy. The mass density of the material is unity.

may be used as follows: A tabular value of absorbed fraction corresponding to a mass m in a unit-density medium will correspond to a mass of m/ρ^2 in a medium of density ρ. This conversion is rigorously correct. The backscatter corrections of Table 12 will also refer to the scaled values of mass, but can be used to give a very approximate correction for backscatter to a region of lower density surrounded by a 70-kg sphere. However, for most organ models involving two media of differing density, it is desirable to perform original Monte Carlo calculations.

Similarly, these tables may be used for materials of slightly different atomic composition by means of conversion based on electron density. If a new material has an electron density (electrons/g) n and the reference material n_o a tabular entry referring to a mass m of the reference material will refer to a mass $(n_o/n)^3 m$ of the new material. However, if the atomic composition differs significantly, it is necessary to perform original Monte Carlo calculations.

If both mass density and composition change, both corrections will apply and the tabular entry will correspond to a mass $(m/\rho^2)\ (n_o/n)^3$. It should be noted that in all cases, the values of absorbed fraction remain constant but the corresponding mass changes.

10. ABSORBED FRACTIONS FOR POINT SOURCES

Table 4 gives values of absorbed fractions as a function of target mass for central-point-source photon emitters. This data is applicable to both elliptical cylinders and ellipsoids containing a central point source (*1*), (see also Fig. 3). The principal axes corresponding to width, thickness and height of these targets are in the ratios of 1/1.8/6.19 and 1/1.8/9.27, respectively. These ratios correspond to 36 cm × 20 cm cross-sectional dimensions for a 70-kg target.

Table 5 gives values of absorbed fractions for central point sources in *bounded* spheres, i.e., without backscatter. As noted above, the absorbed fraction for spheres is greater than that for anatomical models such as elliptical cylinders or ellipsoids of equal mass.

Table 6 presents values of absorbed fractions for central point sources in right circular cylinders. Note that the principal axes corresponding to width, thickness and height of the right circular cylinders used for obtaining the absorbed fraction data of Table 6 are in the ratio 1/1/0.75. The cross-sectional dimensions for these cylinders are different from those of elliptical cylinders of equal mass used in preparing the data given in Table 4. The dimensions of the cylindrical targets used in preparing Table 6 are close to those of spherical targets and have similar values of absorbed fraction (see Fig. 3). For this reason the central point-source absorbed-fraction data for elliptical cylinders given in Table 4 is more useful for clinical applications.

TABLE 8. ABSORBED FRACTIONS FOR POINT SOURCES AT DISTANCES 1/2, 1/6 AND 1/12 HEIGHT OF ELLIPTICAL CYLINDERS*

Mass (kg)	ϕ								
	0.080 MeV			0.662 MeV			2.750 MeV		
	1/2	1/6	1/12	1/2	1/6	1/12	1/2	1/6	1/12
2	0.166	0.158	0.149	0.176	0.165	0.151	0.125	0.116	0.105
4	0.212	0.203	0.187	0.215	0.204	0.186	0.154	0.145	0.133
6	0.247	0.238	0.217	0.242	0.230	0.211	0.174	0.164	0.152
8	0.276	0.266	0.242	0.263	0.250	0.230	0.190	0.179	0.166
10	0.301	0.291	0.264	0.281	0.266	0.245	0.204	0.192	0.178
20	0.388	0.378	0.343	0.340	0.323	0.299	0.251	0.238	0.220
30	0.447	0.437	0.399	0.379	0.361	0.335	0.282	0.268	0.249
40	0.491	0.482	0.442	0.409	0.390	0.362	0.306	0.292	0.271
50	0.527	0.518	0.477	0.433	0.413	0.384	0.325	0.312	0.289
60	0.557	0.548	0.507	0.453	0.434	0.403	0.342	0.328	0.304
70	0.583	0.575	0.533	0.470	0.452	0.419	0.356	0.343	0.318
80	0.606	0.598	0.556	0.486	0.467	0.434	0.369	0.356	0.330
90	0.626	0.618	0.576	0.500	0.482	0.448	0.380	0.368	0.341
100	0.644	0.636	0.595	0.513	0.495	0.460	0.391	0.378	0.351
120	0.674	0.668	0.626	0.535	0.518	0.482	0.409	0.397	0.368
140	0.700	0.694	0.653	0.555	0.537	0.501	0.425	0.413	0.384
160	0.722	0.717	0.676	0.572	0.555	0.518	0.439	0.428	0.397
180	0.740	0.736	0.696	0.587	0.571	0.533	0.452	0.440	0.410
200	0.756	0.753	0.713	0.601	0.585	0.547	0.463	0.451	0.421

* The principal axes of the elliptical cylinders are in the ratio of 1/1.8/6.19.

TABLE 9. ABSORBED FRACTIONS FOR A UNIFORM DISTRIBUTION OF ACTIVITY IN ELLIPSOIDS*

	ϕ										
Mass (kg)	0.020 MeV	0.030 MeV	0.040 MeV	0.060 MeV	0.080 MeV	0.100 MeV	0.160 MeV	0.364 MeV	0.662 MeV	1.460 MeV	2.750 MeV
2	0.702	0.407	0.317	0.131	0.072	0.099	0.113	0.112	0.134	0.099	0.096
4	0.762	0.485	0.325	0.176	0.127	0.133	0.144	0.148	0.155	0.133	0.120
6	0.795	0.529	0.345	0.206	0.157	0.155	0.163	0.170	0.173	0.155	0.134
8	0.815	0.560	0.366	0.228	0.179	0.172	0.178	0.187	0.189	0.171	0.147
10	0.830	0.583	0.385	0.247	0.196	0.185	0.190	0.200	0.202	0.183	0.156
20	0.868	0.649	0.460	0.308	0.250	0.233	0.234	0.245	0.250	0.223	0.187
30	0.884	0.685	0.508	0.346	0.284	0.265	0.264	0.273	0.280	0.248	0.207
40	0.893	0.709	0.541	0.374	0.310	0.290	0.287	0.294	0.301	0.267	0.222
50	0.900	0.727	0.567	0.397	0.332	0.312	0.305	0.312	0.317	0.282	0.235
60	0.905	0.741	0.585	0.416	0.351	0.330	0.321	0.327	0.330	0.294	0.247
70	0.909	0.753	0.600	0.432	0.368	0.346	0.335	0.340	0.341	0.306	0.257
80	0.912	0.763	0.613	0.446	0.383	0.361	0.348	0.351	0.351	0.316	0.265
90	0.916	0.772	0.624	0.459	0.397	0.374	0.359	0.362	0.360	0.325	0.274
100	0.918	0.780	0.634	0.471	0.409	0.386	0.369	0.371	0.368	0.334	0.283
120	0.924	0.793	0.652	0.492	0.431	0.407	0.388	0.389	0.384	0.350	0.298
140	0.929	0.804	0.670	0.511	0.450	0.425	0.405	0.405	0.399	0.364	0.310
160	0.933	0.814	0.688	0.528	0.466	0.440	0.421	0.420	0.415	0.378	0.321
180	0.937	0.821	0.708	0.544	0.480	0.454	0.436	0.433	0.432	0.391	0.331
200	0.940	0.828	0.729	0.559	0.491	0.466	0.451	0.446	0.449	0.403	0.340

* The principal axes of the ellipsoids are in the ratio of 1/1.8/9.27.

TABLE 10. ABSORBED FRACTIONS FOR UNIFORM DISTRIBUTION OF ACTIVITY IN SMALL SPHERES* AND THICK ELLIPSOIDS*

	ϕ										
Mass (kg)	0.020 MeV	0.030 MeV	0.040 MeV	0.060 MeV	0.080 MeV	0.100 MeV	0.160 MeV	0.364 MeV	0.662 MeV	1.460 MeV	2.750 MeV
0.3	0.684	0.357	0.191	0.109	0.086	0.085	0.087	0.099	0.096	0.092	0.077
0.4	0.712	0.388	0.212	0.121	0.096	0.093	0.097	0.108	0.108	0.099	0.083
0.5	0.731	0.412	0.229	0.131	0.104	0.099	0.104	0.116	0.117	0.104	0.089
0.6	0.745	0.431	0.244	0.140	0.111	0.105	0.111	0.122	0.124	0.109	0.093
1.0	0.780	0.486	0.289	0.167	0.135	0.125	0.130	0.142	0.144	0.125	0.106
2.0	0.818	0.559	0.360	0.212	0.173	0.160	0.162	0.174	0.173	0.153	0.127
3.0	0.840	0.600	0.405	0.245	0.201	0.188	0.186	0.197	0.195	0.174	0.143
4.0	0.856	0.629	0.438	0.271	0.222	0.209	0.205	0.216	0.213	0.190	0.156
5.0	0.868	0.652	0.464	0.294	0.241	0.227	0.222	0.231	0.228	0.204	0.167
6.0	0.876	0.671	0.485	0.312	0.258	0.241	0.236	0.245	0.240	0.216	0.177

* The principal axes of the small spheres and thick ellipsoids are in the ratios of 1/1/1 and 1/0.667/1.333.

Table 7 lists the results of calculations that were performed for small right circular cylinders. The tissue formula used in these calculations was ($C_6H_{40}O_{18}N$), the electron density is 3.41×10^{23} electrons/g, and the mass density is unity.

Table 8 lists the values of absorbed fractions for an axial point photon source in elliptical cylinders located at a distance 1/2, 1/6 and 1/12 from the end of the height of the cylinder. The values for the distance of 1/2 the height are the same as in Table 4. These tables illustrate the effect of varying the position of a point source along the axis. The variation is surprisingly small for the rather elongated cylinders used in this calculation. The results indicate that for axial sources within a cylindrical target the absorbed fraction for a central point source may be used for other axial locations with an error of less than 10%.

11. ABSORBED FRACTIONS FOR A UNIFORM DISTRIBUTION OF ACTIVITY

Table 9 lists the absorbed fractions for a uniform distribution of activity in elongated targets. The principal axes corresponding to width, thickness and height of these targets are in the ratio 1/1.8/9.27. These target dimensions are exactly equal to those of the ellipsoidal

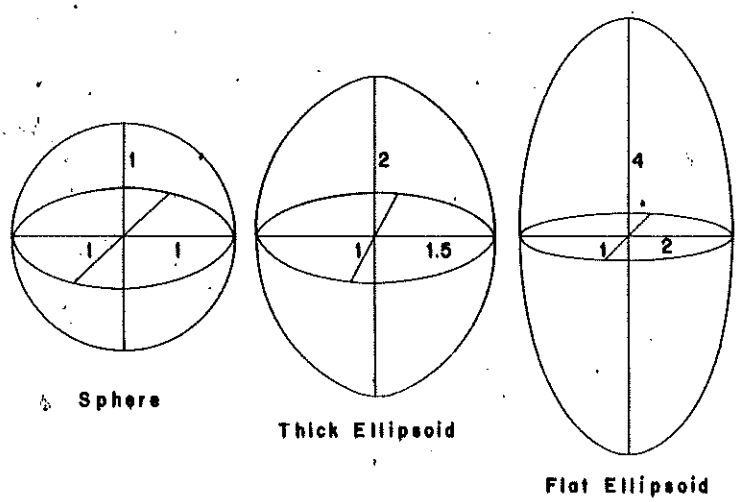

FIG. 6. Models for organs of various shapes used in Tables 10 and 11. (Courtesy of *Brit. J. Radiol.*)

targets used to obtain the point source absorbed fraction data of Table 4.

Tables 10 and 11 give absorbed fractions for small target volumes which may be used as models for organs containing a uniform distribution of activity. The target geometries used in these calculations are shown in Fig. 6. Table 10 lists values applicable to either spheres or thick ellipsoids of masses ranging from 0.3 to 6 kg. In this mass range the difference between spheres and thick ellipsoids of equal mass is very small (*2*). The values given in Table 11 are for flat ellipsoids. The selection of an appropriate target shape (model) must be made with reference to the organ of interest. However, in the mass range considered here, the absorbed fraction for a given mass is a weak function of target shape. Consequently, the absorbed-fraction data listed in Tables 10 and 11 can be used to obtain reasonably accurate values of the absorbed dose in an organ containing a uniform distribution of activity.

TABLE 11. ABSORBED FRACTIONS FOR UNIFORM DISTRIBUTION OF ACTIVITY IN FLAT ELLIPSOIDS*

	ϕ								
Mass (kg)	0.020 MeV	0.030 MeV	0.040 MeV	0.060 MeV	0.080 MeV	0.100 MeV	0.160 MeV	0.662 MeV	2.75 MeV
0.3	0.627	0.306	0.164	0.090	0.075	0.072	0.078	0.084	0.062
0.4	0.654	0.334	0.179	0.098	0.081	0.079	0.085	0.095	0.069
0.5	0.674	0.356	0.192	0.106	0.087	0.085	0.090	0.103	0.074
0.6	0.690	0.374	0.204	0.112	0.092	0.090	0.095	0.109	0.079
1.0	0.731	0.423	0.243	0.134	0.109	0.106	0.112	0.128	0.093
2.0	0.779	0.492	0.305	0.173	0.140	0.133	0.140	0.154	0.112
3.0	0.803	0.533	0.344	0.200	0.162	0.154	0.159	0.171	0.125
4.0	0.820	0.564	0.372	0.221	0.181	0.171	0.174	0.185	0.136
5.0	0.833	0.588	0.394	0.238	0.197	0.185	0.187	0.197	0.146
6.0	0.844	0.608	0.414	0.254	0.211	0.198	0.198	0.209	0.156

* The principal axes of the flat ellipsoids are in the ratio of 1/0.5/2.0.

TABLE 12. FRACTIONAL INCREASE OF ABSORBED FRACTION IN CENTRAL ORGAN DUE TO BACKSCATTERED RADIATION FROM 70-kg PHANTOM SURROUNDING ORGAN

Energy (MeV)	0.020	0.030	0.040	0.060	0.080	0.100	0.160	0.364	0.662	1.46	2.75
Fractional increase of ϕ	1.01	1.08	1.19	1.24	1.28	1.26	1.17	1.05	1.04	1.02	1.01

12. INCREASE IN ABSORBED FRACTION DUE TO BACKSCATTER

Tables 4–11 give the absorbed fractions for targets of finite volume, and these values do not include the contribution due to photons coming from outside the target volume and interacting within it. For the situation where organs are located within the trunk of the body, the average absorbed dose will contain a contribution due to the backscattered photons. Table 12 may be used to obtain the fractional increase in the absorbed dose due to backscatter. This table gives the ratio of the absorbed fraction for activity distributed uniformly in a sphere of 780 g located within a 70-kg spherical target to that of the same sphere in vacuum. Our studies show that the values so obtained are relatively independent of the mass or shape of the organ containing the activity. Also, the amount of backscatter is relatively independent of the exact mass of the scattering volume surrounding the target, provided this scattering medium is much larger than the target volume. Consequently, Table 12 should yield adequate estimates of the increase in absorbed fraction to organs within the trunk of the body due to backscatter.

ACKNOWLEDGMENTS

Many individuals have assisted in various phases of this work. However, M. Wachter and A. Callahan were particularly instrumental in the development of the original Monte Carlo program and the Sort Program.

This project has been supported by the Atomic Energy Commission, the National Institutes of Health and the Office of Naval Research.

The work of the MIRD Committee is supported by U. S. Public Health Service Research Grant RH .00416, National Center for Radiological Health.

REFERENCES

1. ELLETT, W. H., CALLAHAN, A. B. AND BROWNELL, G. L.: Gamma-ray dosimetry of internal emitters. I. Monte Carlo calculations of absorbed dose from point sources. *Brit. J. Radiol.* **37**:45–52, 1964.

2. ELLETT, W. H., CALLAHAN, A. B. AND BROWNELL, G. L.: Gamma-ray dosimetry of internal emitters. II. Monte Carlo calculations of absorbed dose from uniform sources. *Brit. J. Radiol.* **38**:541–544, 1965.

3. REDDY, A. R., ELLETT, W. H. AND BROWNELL, G. L.: Gamma-ray dosimetry of internal emitters. III. Monte Carlo calculations of absorbed dose for low-energy gamma-rays. *Brit. J. Radiol.* **42**:512–515, 1967.

4. LOEVINGER, R. AND BERMAN, M.: MIRD Pamphlet No. 1—A schema for absorbed-dose calculations for biologically distributed radionuclides. *J. Nucl. Med., Suppl. No. 1*, 7, 1968.

5. KAHN, H.: U.S.A.E.C. (RAND) Report, R 1237 April, 1954.

6. GRODSTEIN, G. W.: N.B.S. Circular 583, U.S. Government Printing Office, Washington, D.C., 1957.

7. MCGINNIS, R. T.: Supplement to N.B.S. Circular 583, U.S. Government Printing Office, Washington, D.C., 1959.

8. ELLETT, W. H., BROWNELL, G. L. AND REDDY, A. R.: Assessment of Monte Carlo calculations for determining the gamma ray dose from internal emitters. To be published in *Phys. Med. Biol.* **13**: 1968.

9. BERGER, M. J.: MIRD Pamphlet No. 2—Energy deposition in water by photons from point isotropic sources, *J. Nucl. Med., Suppl. No. 1*, 15, 1968.

10. SNYDER, W. S. AND FORD, M. R.: A Monte Carlo code for estimation of dose from gamma-ray sources, *ORNL–3849*, 1965, pp. 193–195.

11. WALTER S. SNYDER, ORNL, November 1, 1965, personal communication.

12. MAYNEORD, W. V.: Energy absorption IV, The mathematical theory of integral dose in radium therapy. *Brit. J. Radiol.* **18**:12, 1945.

13. LOEVINGER, R., JAPHA, E. M. AND BROWNELL, G. L.: *Radiation dosimetry*, Ed. by Hine, G. J. and Brownell, G. L., Academic Press, New York, 1956, p. 78.